

Imaging mass spectrometry of isotopically-resolved intact proteins on a trapped ion-mobility quadrupole time-of-flight mass spectrometer

Dustin R. Klein^{1,2+}, Emilio S. Rivera^{1,2+}, Richard M. Caprioli^{1,2,3,4,5}, Jeffrey M. Spraggins^{1,2,3,6,7*}

¹Mass Spectrometry Research Center, Vanderbilt University, Nashville, TN 37235, USA

²Department of Biochemistry, Vanderbilt University, Nashville, TN 37235, USA

³Department of Chemistry, Vanderbilt University, Nashville, TN 37235, USA

⁴Department of Medicine, Vanderbilt University, Nashville, TN 37235, USA

⁵Department of Pharmacology, Vanderbilt University, Nashville, TN 37235, USA

⁶Department of Cell and Developmental Biology, Vanderbilt University, Nashville, TN 37235, USA

⁷Department of Pathology, Microbiology, and Immunology, Vanderbilt University Medical Center, Nashville, TN 37235, USA

+Authors contributed equally

*Corresponding Author: Jeffrey M. Spraggins, jeff.spraggins@vanderbilt.edu

Abstract

In this work, we demonstrate rapid, high spatial, and high spectral resolution imaging of intact proteins by matrix-assisted laser desorption/ionization (MALDI) imaging mass spectrometry (IMS) on a hybrid quadrupole-reflectron time-of-flight (qTOF) mass spectrometer equipped with trapped ion mobility spectrometry (TIMS). Historically, untargeted MALDI IMS of proteins has been performed on TOF mass spectrometers. While advances in TOF instrumentation have enabled rapid, high spatial resolution IMS of intact proteins, TOF mass spectrometers generate relatively low-resolution mass spectra with limited mass accuracy. Conversely, the implementation of MALDI sources on high-resolving power Fourier transform (FT) mass spectrometers has allowed IMS experiments to be conducted with high spectral resolution with the caveat of increasingly long data acquisition times. As illustrated here, qTOF mass spectrometers enable protein imaging with the combined advantages of TOF and FT mass spectrometers. Protein isotope distributions were resolved for both a protein standard mixture and proteins detected from a whole-body mouse pup tissue section. Rapid (~10 pixels/s) 10 μm lateral spatial resolution IMS was performed on a rat brain tissue section while maintaining isotopic spectral resolution. Lastly, proof-of-concept MALDI-TIMS data was acquired from a protein mixture to demonstrate the ability to differentiate charge states by ion mobility. These experiments highlight the advantages of qTOF and timsTOF platforms for resolving and interpreting complex protein spectra generated from tissue by IMS.

Introduction

Untargeted biomolecular imaging of tissues has largely been driven by the advancement of imaging mass spectrometry (IMS).¹⁻⁵ During a typical IMS experiment, analytes are sampled and ionized directly from tissue surfaces along a coordinate plane, detected by a mass spectrometer, and visualized as ion heat maps according to ion abundances.⁴ The lateral spatial resolution of an ion image is reported as the tissue area used to represent a single mass spectrum, *i.e.*, one spectrum per pixel. IMS has been used to map distributions of metabolites, lipids, peptides, and proteins, and is complementary to histological methods

(stained and antibody-based imaging).^{4,6,7} Proteins can be analyzed either intact or as peptides generated after on-tissue enzymatic digestion.⁷⁻⁹ While on-tissue digestion strategies expand the range of detectable proteins, biologically relevant proteoform information (e.g., post-translational modifications, protein sequence truncations, point mutations, etc.) is potentially lost.^{10,11} Alternatively, proteoform information is preserved during intact protein analysis; however, the size of detectable proteins is expected to be limited with this approach.

Matrix-assisted laser desorption/ionization (MALDI), which generates low-charge state ions at relatively high mass-to-charge (m/z) ratios, is the most commonly used ionization method for intact protein IMS. Therefore, intact protein MALDI IMS experiments are typically performed using time-of-flight (TOF) mass spectrometers owing to their theoretically unlimited m/z range and high sensitivity. Novel sample preparation techniques and high mass detectors on TOF instruments have enabled the detection of proteins ≥ 50 kDa using TOF platforms.¹²⁻¹⁴ Lui *et al.* recently reported the use of caffeic acid to detect intact proteins from tissue at $m/z \sim 190,000$.¹⁴ In addition, advances in MALDI-TOF instrumentation and laser optics have enabled rapid acquisition of spectra from increasingly small sampling regions¹⁵⁻¹⁸; ion images acquired at a rate of up to 30 pixels/sec with a lateral spatial resolution of 5 μm , have been reported.¹⁷ However, during tissue analysis, the limited mass resolving power of TOF instruments, especially with detection in linear mode, results in convoluted spectra from which few accurate protein and proteoform intact masses can be determined.

Implementing MALDI on Fourier transform-ion cyclotron resonance (FT-ICR) and Orbitrap mass spectrometers has enabled high resolution and mass accuracy measurements for both intact endogenous proteins from tissue and protein standards.^{10,18-23} Historically, FT-ICR and Orbitrap instruments have had lower and narrower m/z ranges by comparison to TOF mass spectrometers, which has restricted intact protein analysis by MALDI on high-resolution instruments. Strategies to overcome m/z range limitations have included manipulation of instrument source pressure and tuning of ion optics for increased ion transmission efficiency²¹, and use of novel matrices to achieve higher charge state ions²³. The advent of an extended m/z range Orbitrap mass spectrometer with an upper range limit of m/z 80,000 also holds promise for intact protein IMS experiments, as was recently demonstrated for spatial mapping of histone proteoforms in human kidney tissue.^{24,25} While the mass spectral characteristics of FT-ICR and Orbitrap mass analyzers are attractive, it is crucial to consider the inverse relationship between m/z and resolving power when performing MALDI IMS on FT-MS systems.²⁶ To achieve resolving powers capable of providing isotopic resolution at high m/z values, increasingly long scan times (i.e., time-domain transient lengths of $\gg 1\text{s}$) are required.²¹ During a MALDI IMS experiment, where tens to hundreds of thousands of spectra are collected, data acquisition times can exceed 24 hours. Experiments are often conducted at lateral spatial resolutions $\geq 75 \mu\text{m}$ or lower mass resolving powers to mitigate the time cost associated with MALDI IMS on FT-MS instruments.²¹ Computational approaches are also being developed to improve protein imaging performance. Image fusion workflows combining data sets from MALDI-TOF and MALDI FT-ICR mass spectrometers have been developed to capitalize on the benefits of each instrument, for example.²⁷

The future of intact protein IMS relies on developing instrumentation that combines speed, high lateral spatial resolution, and high spectral resolution. Hybrid quadrupole-TOF (qTOF) mass spectrometers

possess each of these desirable characteristics and have the potential to combine the benefits of both FT-MS and TOF platforms. Unlike FT-MS systems where instrument resolving power decreases with increasing m/z , TOF and qTOF mass spectrometers have relatively constant resolving powers across the m/z range. Therefore, increased instrument scan times are unnecessary to achieve high mass resolution at high m/z . A recently introduced qTOF mass spectrometer equipped with MALDI source and trapped ion mobility spectrometry (TIMS) was shown to provide rapid spectral acquisition rates (≥ 20 Hz), high lateral spatial resolution (10 μm), and spectral resolution greater than 40,000 for lipid imaging.²⁸ The present work demonstrates the advantages of using this mass spectrometer in qTOF-mode for rapid MALDI IMS of isotopically resolved proteins at high lateral spatial resolution. In addition, proof-of-concept TIMS data for MALDI-generated protein standards shows the potential for further spectral deconvolution during protein IMS.

Experimental

Materials

2,5-dihydroxyacetophenone (DHA) matrix, red phosphorus, and the protein standards ubiquitin (8.6 kDa), thioredoxin (11.6 kDa), apomyoglobin (16.9 kDa), and β -lactoglobulin (18.3 kDa), toluene, and ammonium hydroxide were purchased from Sigma-Aldrich (St. Louis, MO). (E)-4(2,5-dihydroxyphenyl)but-3-en-2-one (2,5-cDHA) was synthesized in-house. Tissues were purchased from BioIVT (Westbury, NY). Indium-tin-oxide (ITO)-coated microscope slides were purchased from Delta Technologies (Loveland, CO). Agilent Tuning mix was purchased from Agilent (Santa Clara, CA). Water, chloroform, acetonitrile, ethyl acetate, acetic acid, and formic acid were purchased from Fisher Scientific (Waltham, MA). Rat brain tissue was purchased from Pel-Freeze Biologicals (Rogers, AR) and stored at -80 °C until analysis.

Sample preparation

For protein standard analysis, a mixture of protein standards [ubiquitin (2 pmol/ μL), apomyoglobin (4 pmol/ μL), thioredoxin (6 pmol/ μL), β -lactoglobulin (8 pmol/ μL)] in water were combined 1:1 with 15 mg/mL DHA in ACN/ H_2O (90:10) with 0.1% formic acid. A series of 1 μL aliquots were deposited onto an MTP AnchorChip MALDI target (Bruker Daltonik, Bremen, Germany) and dried. For imaging experiments, all tissues were sectioned using a CM3050S cryostat from Leica Microsystems (GmbH, Wetzlar, Germany) and thaw-mounted on ITO slides. Rat brain tissues were sectioned at 10 μm thickness. A one-week-old C57BL/6 control mouse pup was snap-frozen at -80 °C, shaved over dry ice, and cryosectioned at a 20 μm thickness. Tissues were coated with cDHA matrix following a previously published method.¹⁷ Briefly, a 3 mg/mL solution of cDHA dissolved in ethyl acetate and toluene (1:1) was applied, followed by a second application of 9 mg/mL solution dissolved in ACN/ H_2O (3:7) with 1% TFA and 0.5% ammonium hydroxide, each using a TM Sprayer (HTX Technologies, LLC, Chapel Hill, NC). Tissues were rehydrated by suspending samples over 1 mL of 50 mM acetic acid for 3 min at 37° C.

Mass Spectrometry and Ion Mobility

All experiments were conducted in positive ion mode on a prototype MALDI timsTOF Pro mass spectrometer (Bruker Daltonik, Bremen, Germany) equipped with a SmartBeam 3D 10 kHz frequency tripled Nd:YAG laser (355 nm) operated with beam scanning on. This instrument will be referred to as a timsTOF fleX throughout this work. Spectra of spotted protein standards in both “qTOF”-mode, where no

ion mobility separation was performed, and TIMS-mode were acquired with a pixel size of 50 μm x 50 μm with 1000 laser shots per pixel. IMS of the whole-body mouse pup was also performed at a pixel size of 50 μm x 50 μm with 1,000 laser shots per pixel. IMS of the rat brain tissue section was performed with a pixel size of 10 μm x 10 μm with 750 laser shots per pixel. For optimal transmission of protein ions, the following instrument parameters were used: ion transfer time = 300 μs ; pre-pulse storage = 50 μs ; collision RF = 4000 V; collision energy = 10 eV; ion energy in the quadrupole = 5 eV; TIMS Funnel 1 RF = 500 Vpp; TIMS Funnel 2 RF = 475 Vpp. For analysis of the protein standard mixture using TIMS, calibration was performed using Agilent Tuning mix. To achieve a reduced mobility ($1/K_0$) range of 0.8 to 5.0, calibration was performed after a series of incremental decreases in the TIMS Tunnel In pressure. An ion mobility separation time of 200 ms and a reduced mobility ($1/K_0$) range of 0.8 to 5.0 were used. Bruker Data Analysis software and SCiLS Lab Version 2020 (Bruker Daltonics, Bremen, Germany) were used to analyze data and generate ion images.

Results

The feasibility of high m/z detection and calibration was assessed here via MALDI-generated ions using red phosphorus, an analyte that produces a predictable series of clusters upon laser irradiation. The scan range of the instrument was set to m/z 2,000 – 20,000 (**Figure S1**). The pre-pulse storage and ion transfer time were adjusted to 50 and 300 μs , respectively, to allow for the transmission of higher m/z ions. Ions were detected up to m/z \sim 17,000, confirming that this system can be tuned to detect high m/z ions and that red phosphorus ions are a suitable calibration standard for this platform over a wide mass range. **Table S1** shows the list of detected red phosphorus ions that were used for calibration. MALDI has been previously utilized on the timsTOF fleX for analyzing metabolites²⁹, lipids²⁸, and glycans³⁰, where ions were detected up to m/z 4,000. The detection of ion with m/z \sim 17,000 far exceeds these previous results and is comparable to work published by Fernandez-Lima and co-workers, where they used a modified timsTOF Pro to detect ESI-generated oligomer ions from a calibration standard up to m/z 19,000.³¹

To assess instrument performance for intact proteins, MALDI spectra were collected for a protein mixture containing ubiquitin, thioredoxin, apomyoglobin, and β -lactoglobulin with a range of m/z 2,000-20,000 (**Figure 1, Figure S2, Table S2**). Data represented in **Figures 1** and **S2** are averages of 50 spectra. A range of charge states are observed for each protein, including the $[\text{M}+\text{H}]^+$ ion of β -lactoglobulin detected at over m/z 18,000. Like previous work conducted by Prentice et al. on a MALDI FT-ICR mass spectrometer, the influence of instrument source pressure on mass range and protein charge state intensities was evaluated by adjusting the TIMS tunnel pressure (determined by the TIMS Tunnel In Pressure instrument reading, **Figure S2**). For ease of spectral comparison, the spectrum from **Figure 1a** showing the MALDI mass spectrum at a TIMS tunnel pressure of 1.5 mBar is included in **Figure S2** as **Figure S2g**. Similar to the results reported by Prentice et al. for decreasing ion funnel pressure, reducing TIMS tunnel pressure increases higher m/z ion intensity. For example, at a TIMS tunnel pressure of 2.6 mbar, which is considered the normal operating pressure for typical proteomic and lipidomic workflows, the $[\text{M}+\text{H}]^+$ charge states of apomyoglobin and β -lactoglobulin at m/z 16,000 and m/z 18,000, respectively, are nearly indistinguishable from the instrument noise. With decreasing TIMS tunnel pressure, a gradual increase in signal intensity is observed for singly charged ions. These results are consistent with results recently presented in a Bruker Daltonics technical note.³² Consequently, all qTOF-only experiments were

conducted at 1.5 mBar, the lowest TIMS tunnel pressure setting. **Figures 1b-i** contain a series of expanded spectra for the $[M+H]^+$ and $[M+2H]^{2+}$ charge states of each protein in the protein standard mixture. Protein signals are isotopically resolved for all charge states, as expected for a constant instrument resolving power of $\sim 40,000$ across the m/z range. In addition, calculated ppm error values for the most intense isotopes of the $[M+H]^+$ and $[M+2H]^{2+}$ ions for each protein are < 5 ppm. (Sequences for protein standards are provided in **Table S2**.) Notably, this data is comparable to that collected on an FT-ICR mass spectrometer during a MALDI protein imaging experiment.²¹

The high mass resolution, accurate mass MALDI spectra collected for protein standards confirms the suitability of the timsTOF fleX for intact protein analysis. Using the same method, protein IMS was performed on a tissue section of a whole-body mouse pup with a lateral spatial resolution of $50\ \mu\text{m}$. **Figure 2a** depicts individual and overlaid ion images for m/z 4,963.4, m/z 8,451.5, m/z 11,306.6, and m/z 12,724.6. Ion images are generated from the most intense individual peak from each isotope distribution. Averaged spectra extracted from specific anatomical features (outlined with dotted yellow lines) are shown in **Figures 2b-e**. Insets within **Figures 2b-e** show expanded spectra for each imaged m/z value and confirm baseline isotopic resolution was achieved across the measured m/z range. The ions of m/z 4,963.4 and m/z 11,306.6 were identified as thymosin- β 4 and histone H4 based on mass accuracy. An average spectrum across the entire mouse pup section is shown in **Figure S3**, and additional individual ion images for other m/z values are shown in **Figure S4**.

Previous work on the timsTOF fleX demonstrated that lipid imaging could be conducted with a lateral spatial resolution of $10\ \mu\text{m}$.²⁸ To evaluate the potential for imaging of intact proteins at $10\ \mu\text{m}$, protein IMS was performed on an axial rat brain tissue section (**Figure 3**). Overlaid ion images of m/z 13,701.6 and m/z 14,112.1 localizing to the granular cell layer and white matter, respectively, confirm that $10\ \mu\text{m}$ protein IMS data can be collected on the timsTOF fleX. To compensate for the lower signal intensities that result from sampling smaller areas, ion images here were generated from entire isotope distributions. The ion image in **Figure 3** contains 178,590 pixels and took 4.6 hours to collect, corresponding to a scan rate of ~ 10 pixels per second. For comparison, to theoretically collect $\sim 178,000$ pixels on a 15 T FT-ICR mass spectrometer with a spectral resolving power of 40,000 at $m/z \sim 14,000$ would take approximately 145 hours (**Equations S1 and S2**). Collection of MALDI IMS data on a qTOF mass spectrometer, therefore, provides $>30\times$ improvement in time savings without sacrificing instrument resolving power compared to FT-MS platforms.

With the analysis of increasingly complex mixtures, separation before mass analysis can be beneficial. Incorporating ion mobility into IMS experiments to provide a dimension of separation orthogonal to m/z has become increasingly popular. For example, TIMS has been utilized to separate lipid isobars during MALDI IMS analysis^{28,29}, and field asymmetric ion mobility spectrometry (FAIMS) has been used during LESA-IMS to increase the number of detectable proteins³³. **Figure 4a** shows a heat map of m/z vs. the inverse of the reduced mobility ($1/K_0$) obtained during MALDI-TIMS analysis of the protein standard mixture. Consistent with previously reported ion mobility data, TIMS provides charge state separation in the form of trendlines, with higher charge state ions having lower $1/K_0$ values.³¹ **Figure 4b** shows overlaid mass spectra extracted from each region circled in the m/z - $1/K_0$ heat map. When performing TIMS separations, the highest m/z values detected were around m/z 9,000. In the future, adjusting ion optic RF

frequencies and additional instrument tuning may provide a means to increase ion transmission efficiency for higher m/z ions during TIMS experiments.

Conclusions

This work demonstrates that untargeted protein IMS performed on a qTOF mass spectrometer enables rapid, high lateral spatial resolution imaging without sacrificing spectral resolving power. In addition, preliminary studies showed the potential for TIMS to simplify analysis by separating proteins based on charge state. Despite the clear benefits of protein IMS on a qTOF mass spectrometer, protein identification remains challenging. While top-down tandem mass spectrometry (MS/MS) is typically the method of choice for intact protein characterization, two instrument attributes must be considered for MALDI-generated ions on a qTOF: 1) the upper m/z limit for ion isolation and 2) the available ion activation methods. Adjustment of ion optic and quadrupole RF frequencies can potentially extend the upper m/z limit of ion isolation. After ion isolation, producing informative fragment ions during MS/MS is crucial to analyte identification. Low-energy collisional activation, the most commonly used ion activation on qTOF instruments, yields few informative fragment ions for low-charge state ions. Alternative ion activation methods, including ultraviolet photodissociation (UVPD), have previously been shown to provide increased protein sequence coverage for singly-charged ions generated by MALDI.¹⁹ Future implementation of UVPD on a MALDI-qTOF mass spectrometer may benefit *in situ* protein identification, providing much needed capabilities for untargeted, discovery-based spatial proteomics analysis. In summary, the reduced data acquisition time afforded by performing protein MALDI IMS on a qTOF mass spectrometer lowers the barrier to routine collection of high spatial and spectral resolution protein IMS data. Importantly, developing methods using a common MALDI qTOF platform provides a starting point for the entire IMS community to advance the field of spatial proteomics.

Associated Content

The Supporting Information is available free of charge on the ACS Publications website.

Figure S1. MALDI mass spectrum of red phosphorus; Figure S2. MALDI mass spectra of the protein standard as varying TIMS Funnel In pressures; Figure S3. MALDI mass spectrum averaged across the entire mouse pup tissue section; Figure S4. Mouse pup ion images; Table S1. List of red phosphorus ions used for instrument calibration; Table S2. Table of protein standards, including amino acid sequences; Equation S1. Equation for theoretical spectral acquisition time on a 15T FT ICR; Equation S2. Equation for theoretical total acquisition time for a 170,000 pixel MALDI IMS image on a 15T FT-ICR.

Author Information

Corresponding Author

Jeffrey M. Spraggins – Mass Spectrometry Research Center, Department of Chemistry, Department of Biochemistry, and Department of Cell and Developmental Biology, Vanderbilt University, Nashville, Tennessee 37235, United States; orcid.org/0000-0001-9198-5498; Email: jeff.spraggins@vanderbilt.edu

Authors

Dustin R. Klein – Mass Spectrometry Research Center, Department of Biochemistry, Vanderbilt University,

Nashville, Tennessee 37235, United States; orcid.org/0000-0001-7327-6479

Emilio S. Rivera – Mass Spectrometry Research Center, Department of Biochemistry, Vanderbilt University, Nashville, Tennessee 37235, United States; orcid.org/0000-0003-3215-1092

Richard M. Caprioli – Mass Spectrometry Research Center, Department of Chemistry, Department of Biochemistry, Department of Medicine, and Department of Pharmacology, Vanderbilt University, Nashville, Tennessee 37235, United States;

Author Contributions

[†]D.R.K and E.S.R. contributed equally to this work.

Notes

The authors declare no competing financial interest.

Acknowledgments

Support was provided by The National Science Foundation Major Research Instrument Program (CBET – 1828299 awarded to J.M.S. and R.M.C) and the National Institutes of Health (NIH), including grants U54 DK134302 (awarded to J.M.S. and R.M.C), R01 AG078803 (awarded to J.M.S.), 1U54 EY032442 (awarded to J.M.S. and R.M.C). The authors would like to thank Terry Dermody from the University of Pittsburgh for providing the mouse pup, and Daniel Ryan and Katerina Djambazova for assistance with sample preparation and cryosectioning. The authors would also like to thank Mark Ridgeway of Bruker Daltonics for useful discussions and assistance with initial instrument tuning.

References

- (1) Caprioli, R. M.; Farmer, T. B.; Gile, J. Molecular Imaging of Biological Samples: Localization of Peptides and Proteins Using MALDI-TOF MS. *Analytical Chemistry* **1997**, *69* (23), 4751–4760. <https://doi.org/10.1021/ac970888i>.
- (2) Aichler, M.; Walch, A. MALDI Imaging Mass Spectrometry: Current Frontiers and Perspectives in Pathology Research and Practice. *Laboratory Investigation* **2015**, *95* (4), 422–431. <https://doi.org/10.1038/labinvest.2014.156>.
- (3) Caprioli, R. M. Imaging Mass Spectrometry: A Perspective. *Journal of Biomolecular Techniques* **2019**, *30* (1), 7–11. <https://doi.org/10.7171/jbt.19-3001-002>.
- (4) Buchberger, A. R.; DeLaney, K.; Johnson, J.; Li, L. Mass Spectrometry Imaging: A Review of Emerging Advancements and Future Insights. *Analytical Chemistry* **2018**, *90* (1), 240–265. <https://doi.org/10.1021/acs.analchem.7b04733>.
- (5) Tuck, M.; Blanc, L.; Touti, R.; Patterson, N. H.; Nu, S. Van; Villette, S.; Taveau, J.; Ro, A.; Brunelle, A.; Lecomte, S.; Desbenoit, N. Multimodal Imaging Based on Vibrational Spectroscopies and Mass Spectrometry Imaging Applied to Biological Tissue: A Multiscale and Multiomics Review. **2021**. <https://doi.org/10.1021/acs.analchem.0c04595>.
- (6) Berry, K. A. Z.; Hankin, J. A.; Barkley, R. M.; Spraggins, J. M.; Caprioli, R. M.; Murphy, R. C. MALDI Imaging of Lipid Biochemistry in Tissues by Mass Spectrometry. *Chemical reviews* **2011**, *111* (10), 6491. <https://doi.org/10.1021/CR200280P>.

- (7) Spengler, B. Mass Spectrometry Imaging of Biomolecular Information. *Analytical Chemistry* **2015**, *87* (1), 64–82. <https://doi.org/10.1021/ac504543v>.
- (8) Cillero-Pastor, B.; Heeren, R. M. A. Matrix-Assisted Laser Desorption Ionization Mass Spectrometry Imaging for Peptide and Protein Analyses: A Critical Review of on-Tissue Digestion. *Journal of Proteome Research* **2014**, *13* (2), 325–335. <https://doi.org/10.1021/pr400743a>.
- (9) Han, J.; Permentier, H.; Bischoff, R.; Groothuis, G.; Casini, A.; Horvatovich, P. Imaging of Protein Distribution in Tissues Using Mass Spectrometry: An Interdisciplinary Challenge. *TrAC - Trends in Analytical Chemistry* **2019**, *112*, 13–28. <https://doi.org/10.1016/j.trac.2018.12.016>.
- (10) Spraggins, J. M.; Rizzo, D. G.; Moore, J. L.; Rose, K. L.; Hammer, N. D.; Skaar, E. P.; Caprioli, R. M. MALDI FTICR IMS of Intact Proteins: Using Mass Accuracy to Link Protein Images with Proteomics Data. *Journal of the American Society for Mass Spectrometry* **2015**, *26* (6), 947–985. <https://doi.org/10.1007/s13361-015-1147-5>.
- (11) Gregorich, Z. R.; Ge, Y. Top-down Proteomics in Health and Disease: Challenges and Opportunities. *Proteomics* **2014**, *14* (10), 1195–1210. <https://doi.org/10.1002/pmic.201300432>.
- (12) van Remoortere, A.; Zeijl, J. M. Van; Oever, V. Den. MALDI Imaging and Profiling MS of Higher Mass Proteins from Tissue. *Journal of the American Society for Mass Spectrometry* **2010**, *21* (11), 62–66.
- (13) Mainini, V.; Bovo, G.; Chinello, C.; Gianazza, E.; Grasso, M.; Cattoretti, G.; Magni, F. Detection of High Molecular Weight Proteins by MALDI Imaging Mass Spectrometry. *Molecular BioSystems* **2013**, *9* (6), 1101–1107. <https://doi.org/10.1039/c2mb25296a>.
- (14) Liu, H.; Han, M.; Li, J.; Qin, L.; Chen, L.; Hao, Q.; Jiang, D.; Chen, D.; Ji, Y.; Han, H.; Long, C.; Zhou, Y.; Feng, J.; Wang, X. A Caffeic Acid Matrix Improves In Situ Detection and Imaging of Proteins with High Molecular Weight Close to 200,000 Da in Tissues by Matrix-Assisted Laser Desorption/Ionization Mass Spectrometry Imaging. *Analytical Chemistry* **2021**, *93* (35), 11920–11928. <https://doi.org/10.1021/acs.analchem.0c05480>.
- (15) Spraggins, J. M.; Caprioli, R. M. High-Speed MALDI-TOF Imaging Mass Spectrometry: Rapid Ion Image Acquisition and Considerations for next Generation Instrumentation. *Journal of the American Society for Mass Spectrometry* **2011**, *22* (6), 1022–1031. <https://doi.org/10.1007/s13361-011-0121-0>.
- (16) Ogrinc Potočnik, N.; Porta, T.; Becker, M.; Heeren, R. M. A.; Ellis, S. R. Use of Advantageous, Volatile Matrices Enabled by next-Generation High-Speed Matrix-Assisted Laser Desorption/Ionization Time-of-Flight Imaging Employing a Scanning Laser Beam. *Rapid Communications in Mass Spectrometry* **2015**, *29* (23), 2195–2203. <https://doi.org/10.1002/rcm.7379>.
- (17) Yang, J.; Norris, J. L.; Caprioli, R. Novel Vacuum Stable Ketone-Based Matrices for High Spatial Resolution MALDI Imaging Mass Spectrometry. *Journal of Mass Spectrometry* **2018**, *53* (10), 1005–1012. <https://doi.org/10.1002/jms.4277>.

- (18) Spraggins, J. M.; Rizzo, D. G.; Moore, J. L.; Noto, M. J.; Skaar, E. P.; Caprioli, R. M. Next-Generation Technologies for Spatial Proteomics: Integrating Ultra-High Speed MALDI-TOF and High Mass Resolution MALDI FTICR Imaging Mass Spectrometry for Protein Analysis. *Proteomics* **2016**, *16* (11–12), 1678–1689. <https://doi.org/10.1002/pmic.201600003>.
- (19) Dilillo, M.; De Graaf, E. L.; Yadav, A.; Belov, M. E.; McDonnell, L. A. Ultraviolet Photodissociation of ESI- and MALDI-Generated Protein Ions on a Q-Exactive Mass Spectrometer. *Journal of Proteome Research* **2019**, *18* (1), 557–564. <https://doi.org/10.1021/acs.jproteome.8b00896>.
- (20) Nicolardi, S.; Switzar, L.; Deelder, A. M.; Palmblad, M.; Van Der Burgt, Y. E. M. Top-Down MALDI-In-Source Decay-FTICR Mass Spectrometry of Isotopically Resolved Proteins. *Analytical Chemistry* **2015**, *87* (6), 3429–3437. <https://doi.org/10.1021/ac504708y>.
- (21) Prentice, B. M.; Ryan, D. J.; Van De Plas, R.; Caprioli, R. M.; Spraggins, J. M. Enhanced Ion Transmission Efficiency up to m/z 24 000 for MALDI Protein Imaging Mass Spectrometry. *Analytical Chemistry* **2018**, *90* (8), 5090–5099. <https://doi.org/10.1021/acs.analchem.7b05105>.
- (22) Dilillo, M.; Ait-Belkacem, R.; Esteve, C.; Pellegrini, D.; Nicolardi, S.; Costa, M.; Vannini, E.; De Graaf, E. L.; Caleo, M.; McDonnell, L. A. Ultra-High Mass Resolution MALDI Imaging Mass Spectrometry of Proteins and Metabolites in a Mouse Model of Glioblastoma. *Scientific Reports* **2017**, *7* (1), 1–11. <https://doi.org/10.1038/s41598-017-00703-w>.
- (23) Chen, B.; Lietz, C. B.; Li, L. In Situ Characterization of Proteins Using Laserspray Ionization on a High-Performance MALDI-LTQ-Orbitrap Mass Spectrometer. *Journal of the American Society for Mass Spectrometry* **2014**, *25* (12), 2177–2180. <https://doi.org/10.1007/s13361-014-0986-9>.
- (24) Fort, K. L.; Van De Waterbeemd, M.; Boll, D.; Reinhardt-Szyba, M.; Belov, M. E.; Sasaki, E.; Zschoche, R.; Hilvert, D.; Makarov, A. A.; Heck, A. J. R. Expanding the Structural Analysis Capabilities on an Orbitrap-Based Mass Spectrometer for Large Macromolecular Complexes. *Analyst* **2018**, *143* (1), 100–105. <https://doi.org/10.1039/c7an01629h>.
- (25) Zemaitis, K.; Veličković, D.; Kew, W.; Fort, K. L.; Reinhardt-Szyba, M.; Pamreddy, A.; Ding, Y.; Kaushik, D.; Sharma, K.; Makarov, A. A.; Zhou, M.; Paša-Tolić, L. Enhanced Spatial Mapping of Histone Proteoforms in Human Kidney Through MALDI-MSI by High-Field UHMR Orbitrap Detection. *Analytical Chemistry* **2022**, *94*, 12604–12613. <https://doi.org/10.1021/acs.analchem.2c01034>.
- (26) Zubarev, R. A.; Makarov, A. Orbitrap Mass Spectrometry. *Analytical Chemistry* **2013**, *85* (11), 5288–5296. <https://doi.org/10.1021/ac4001223>.
- (27) Spraggins, J. M.; Van de Plas, R.; Moore, J. L.; Ryan, D. J.; Caprioli, R. M. Maximizing Performance of Spatial Proteomics through the Fusion of Ultra-High Speed MALDI-TOF and High Mass Resolution MALDI FTICR IMS. In *Proceedings of the 64th ASMS Conference on Mass Spectrometry and Allied Topics*; San Antonio, 2016.
- (28) Spraggins, J. M.; Djambazova, K. V.; Rivera, E. S.; Migas, L. G.; Neumann, E. K.; Fuetterer, A.; Suetering, J.; Goedecke, N.; Ly, A.; Van De Plas, R.; Caprioli, R. M. High-Performance Molecular Imaging with MALDI Trapped Ion-Mobility Time-of-Flight (TimsTOF) Mass Spectrometry.

- Analytical Chemistry* **2019**, *91* (22), 14552–14560.
<https://doi.org/10.1021/acs.analchem.9b03612>.
- (29) Djambazova, K. V.; Klein, D. R.; Migas, L. G.; Neumann, E. K.; Rivera, E. S.; Van de Plas, R.; Caprioli, R. M.; Spraggins, J. M. Resolving the Complexity of Spatial Lipidomics Using MALDI TIMS Imaging Mass Spectrometry. *Analytical Chemistry* **2020**. <https://doi.org/10.1021/acs.analchem.0c02520>.
- (30) McDowell, C. T.; Klamer, Z.; Hall, J.; West, C. A.; Wisniewski, L.; Powers, T. W.; Angel, P. M.; Mehta, A. S.; Lewin, D. N.; Haab, B. B.; Drake, R. R. Imaging Mass Spectrometry and Lectin Analysis of N-Linked Glycans in Carbohydrate Antigen-Defined Pancreatic Cancer Tissues. *Molecular and Cellular Proteomics* **2021**, *20*, 100012.
<https://doi.org/10.1074/MCP.RA120.002256>.
- (31) Jeanne Dit Fouque, K.; Garabedian, A.; Leng, F.; Tse-Dinh, Y. C.; Ridgeway, M. E.; Park, M. A.; Fernandez-Lima, F. Trapped Ion Mobility Spectrometry of Native Macromolecular Assemblies. *Analytical Chemistry* **2021**, *93* (5), 2933–2941. <https://doi.org/10.1021/acs.analchem.0c04556>.
- (32) Asperger, A.; Goedecke, N. Developing a timsTOF fleX method for enhanced sensitivity in higher m/z MALDI-MS measurements. *Bruker Application Note TN-57* **2023**.
- (33) Griffiths, R. L.; Hughes, J. W.; Abbatiello, S. E.; Belford, M. W.; Styles, I. B.; Cooper, H. J. Comprehensive LESA Mass Spectrometry Imaging of Intact Proteins by Integration of Cylindrical FAIMS. *Analytical Chemistry* **2020**, *92* (4), 2885–2890.
<https://doi.org/10.1021/acs.analchem.9b05124>.

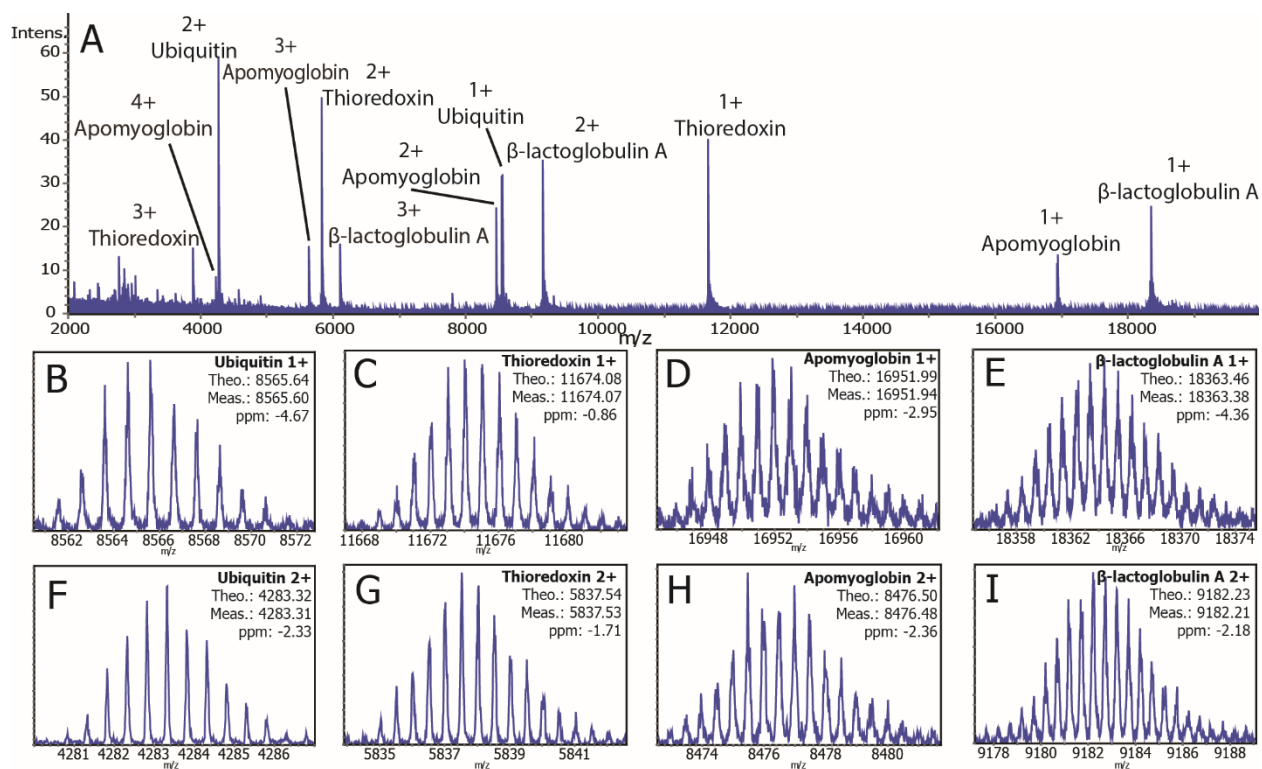


Figure 1. MALDI mass spectrum of a protein standard mixture composed of ubiquitin (8.6 kDa), thioredoxin (11.6 kDa), apomyoglobin (16.9 kDa), and β -lactoglobulin (18.3 kDa) (A) with expanded insets of the $[M+H]^+$ (B-E) and $[M+2H]^{2+}$ (F-I) charge states. A range of charge states are detected for each protein, and all protein ions in the $[M+H]^+$ and $[M+2H]^{2+}$ can be isotopically resolved.

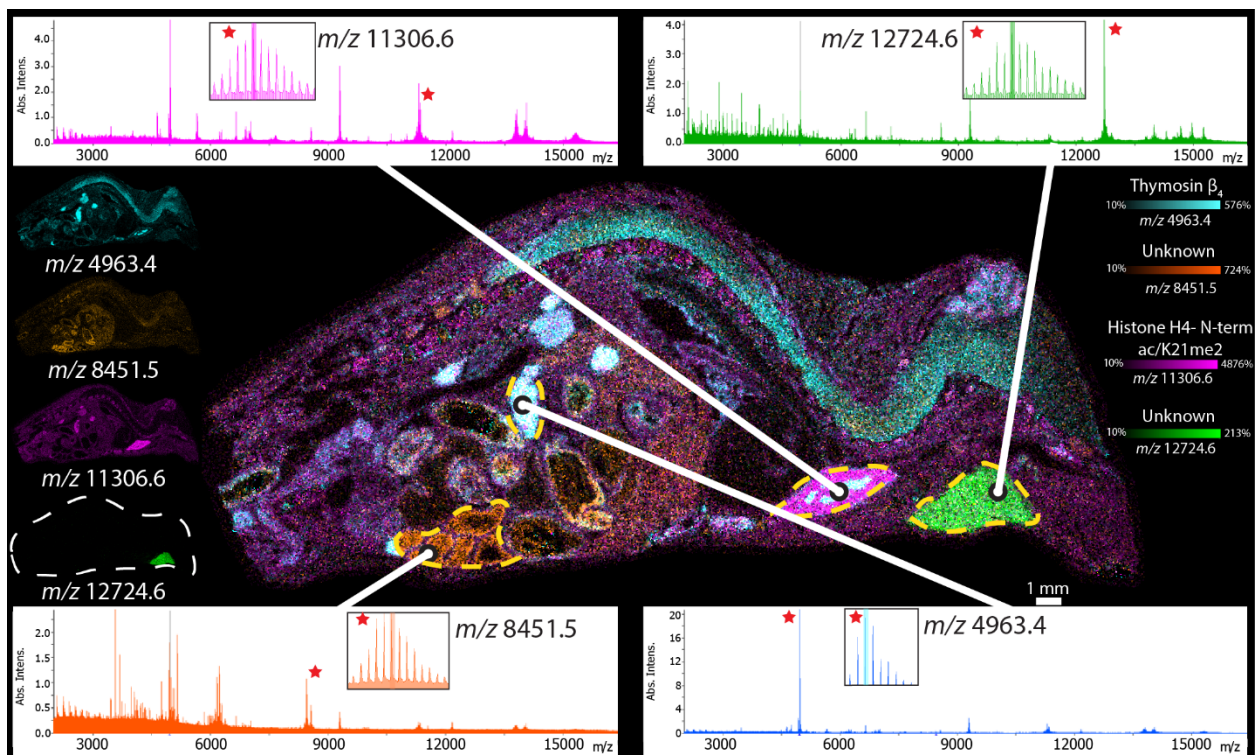


Figure 2. Intact protein IMS performed on a mouse pup tissue. Individual and overlaid ion images of m/z 4,963.4, m/z 8,451.5, m/z 11,306.6, and m/z 12,724.6 show distinct localization of proteins to anatomical features. Averaged mass spectra are shown for regions surrounded by a dotted yellow line. Peaks used to generate ion images are labeled with a red star, and expanded insets are used to show protein ions with resolved isotope distributions.

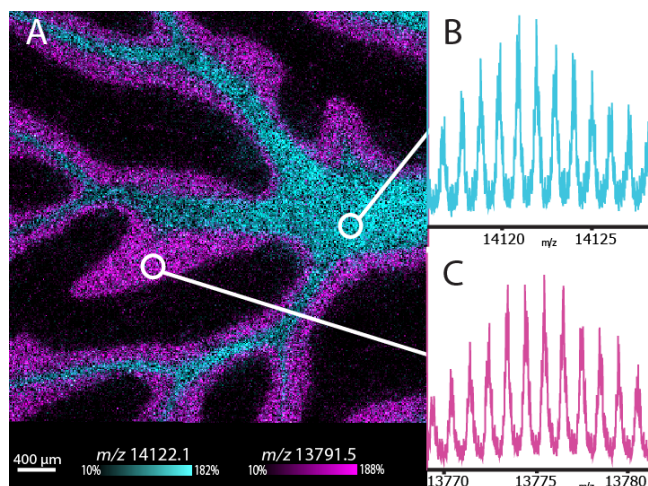


Figure 3. 10 μm protein IMS of rat brain tissue. Overlaid ion images of m/z 14,122.1 and m/z 13,791.5 show that high lateral spatial resolution is possible on the timsTOF fleX (A). Expanded mass spectra of protein isotope distributions (B and C) confirm that high lateral spatial resolution can be performed without compromising mass spectral resolution. Mass spectra are averages generated from regions of interest drawn within each morphological structure (7914 spectra for A and 9507 pixels for B).

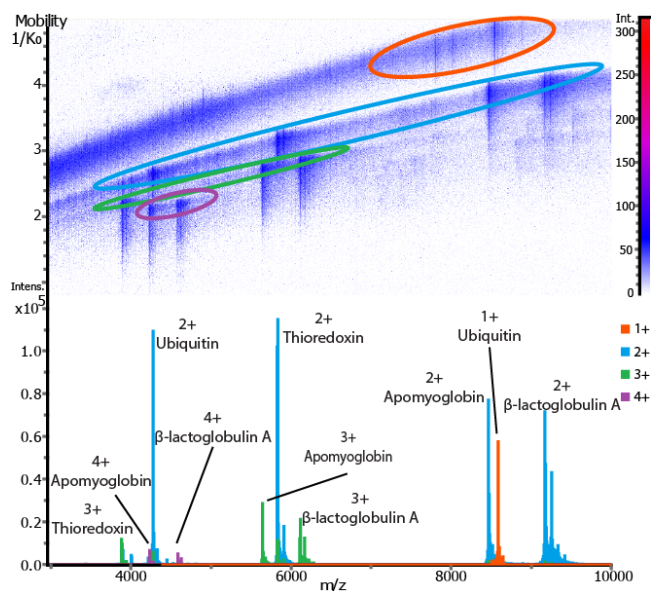


Figure 4. Integration of TIMS allows for the separation of intact protein ions along charge state trendlines. The m/z - $1/K_0$ heat map contains a series of colored circles corresponding to charge state trendlines. Spectra extracted in the bottom portion of this figure are color-coded according to these circled regions and overlaid.